



Tran, M., Zaggoulos, G., Nix, A. R., & Doufexi, A. (2008). Mobile WiMAX: performance analysis and comparison with experimental results. IEEE 68th Vehicular Technology Conference, 2008 (VTC 2008-Fall), 1 - 5.
10.1109/VETEFCF.2008.438

Link to published version (if available):
10.1109/VETEFCF.2008.438

[Link to publication record in Explore Bristol Research](#)
PDF-document

University of Bristol - Explore Bristol Research

General rights

This document is made available in accordance with publisher policies. Please cite only the published version using the reference above. Full terms of use are available:
<http://www.bristol.ac.uk/pure/about/ebr-terms.html>

Take down policy

Explore Bristol Research is a digital archive and the intention is that deposited content should not be removed. However, if you believe that this version of the work breaches copyright law please contact open-access@bristol.ac.uk and include the following information in your message:

- Your contact details
- Bibliographic details for the item, including a URL
- An outline of the nature of the complaint

On receipt of your message the Open Access Team will immediately investigate your claim, make an initial judgement of the validity of the claim and, where appropriate, withdraw the item in question from public view.

Mobile WiMAX: Performance Analysis and Comparison with Experimental Results

Mai Tran, George Zaggoulos, Andrew Nix and Angela Doufexi
Centre for Communications Research, University of Bristol
Bristol, United Kingdom

Abstract— The demand for broadband mobile services continues to grow. Conventional high-speed broadband solutions are based on wired-access technologies such as digital subscriber line (DSL). This type of solution is difficult to deploy in remote rural areas, and furthermore it lacks support for terminal mobility. Mobile Broadband Wireless Access (BWA) offers a flexible and cost-effective solution to these problems. In recent years the WiMAX standard has emerged to harmonise the wide variety of different BWA technologies. The first WiMAX version was based on the IEEE 802.16-2004 standard and offered wireless links to fixed subscribers. The most recent 802.16e standard supports broadband applications to mobile handsets and laptops. This paper analyses the performance of a mobile WiMAX system operating on all link-speeds in an urban microcell. The simulation results are generated using a fully compliant 802.16e simulator and cover important aspects such as link adaptation, packet error rate and throughput. The theory is supported by experimental data captured in an urban microcell environment using a mobile WiMAX basestation. Predicted results are compared with measured data taken from a number of vehicular drive tests. Analysis shows that mobile WiMAX is able to achieve a street-level range of 300-2100m depending on the permitted EIRP level.

Keywords- IEEE 802.16e, BWA, Mobile WiMAX

I. INTRODUCTION

The first WiMAX system (IEEE 802.16-2004) offered fixed broadband wireless communications using rooftop mounted Customer Premises Equipment (CPE) [1]. In December, 2005 the IEEE completed the 802.16e-2005 [2] amendment, which added new features to support mobile applications. The resulting standard is commonly known as mobile WiMAX.

The original WiMAX physical layer (PHY) used orthogonal frequency division multiplexing (OFDM). This provides strong performance in multipath and non-line-of-sight (NLOS) environments. Mobile WiMAX extends the OFDM PHY layer to support terminal mobility and multiple-access. The resulting technology is known as scalable OFDMA. Data streams to and from individual users are multiplexed to groups of subchannels on the downlink and uplink. By adopting a scalable PHY architecture, mobile WiMAX is able to support a wide range of bandwidths. The scalability is implemented by varying the FFT size from 128 to 512, 1024, and 2048 to support channel bandwidths of 1.25 MHz, 5 MHz, 10 MHz, and 20 MHz respectively. Since bandwidth availability is always limited, and user data rate expectations continue to rise, spectral efficiency is key. The random fluctuations of the time-

varying radio channel make the continuous use of high bandwidth efficiency schemes, such as 64QAM, difficult to achieve. To overcome this limitation, Adaptive Modulation and Coding (AMC) is employed to dynamically select the best modulation scheme given knowledge of the radio channel. On a per-link basis, this maintains the highest possible bandwidth efficiency under all operating conditions.

This paper analyses the packet error rate (PER) and throughput performance of mobile WiMAX as a function of signal-to-noise-ratio (SNR) in an urban microcell. The work also determines the SNR switching points between each link-speed. The theoretic performance is compared against practical measurements from a number of mobile drive tests in an urban microcell.

The paper is organized as follows: a description of our Downlink (DL) mobile WiMAX physical layer simulator is given in section II. The underlying wideband channel model is described in section III. Section IV presents the downlink performance in terms of PER and throughput as a function of SNR and link-speed. The configuration of the WiMAX hardware used in the experiments is described in section V. Finally, a comparison is provided between the experimental vehicular results and the predicted theoretic performance.

II. MOBILE WiMAX PHY DESCRIPTION

The mobile WiMAX standard builds on the principles of OFDM by adopting a Scalable OFDMA-based PHY layer (SOFDMA). SOFDMA supports a wide range of operating bandwidths to flexibly address the need for various spectrum allocation and application requirements. When the operating bandwidth increases, the FFT size is also increased to maintain a fixed subcarrier frequency spacing of 10.94 kHz. This ensures a fixed OFDMA symbol duration. Since the basic resource unit (i.e. the OFDMA symbol duration) is fixed, the impact of bandwidth scaling is minimized to the upper layers. Table I shows the relevant parameters for the OFDMA PHY.

TABLE I. OFDMA PHY PARAMETERS

Parameter	Value			
FFT size	128	512	1024	2048
Channel bandwidth (MHz)	1.25	5	10	20
Subcarrier frequency spacing (kHz)	10.94			
Useful symbol period (μs)	91.4			
Guard Time	1/32, 1/16, 1/8, 1/4			

Table II summarises the OFDMA parameters used in our Mobile WiMAX simulator. Fig. 1 shows the transmitter block diagram for the mobile WiMAX simulator used in this paper.

TABLE II. OFDMA PARAMETERS

Parameter	Value	
Channel bandwidth (MHz)	5	
Sampling frequency F_s (MHz)	5.6	
Sampling period $1/F_s$ (μ s)	0.18	
Subcarrier frequency spacing $\Delta f = F_s/N_{FFT}$ (kHz)	10.94	
Useful symbol period $T_b = 1/\Delta f$ (μ s)	91.4	
Guard Time $T_g = T_b/8$ (μ s)	11.4	
OFDMA symbol duration $T_s = T_b + T_g$ (μ s)	102.9	
	DL PUSC	UL PUSC
Number of used subcarriers (N_{used})	421	409
Number of pilot subcarriers	60	136
Number of data subcarriers	360	272
Number of data subcarriers/subchannel	24	16
Number of subchannels	15	17
Number of users (N_{users})	3	3
Number of subchannels/user	5	4

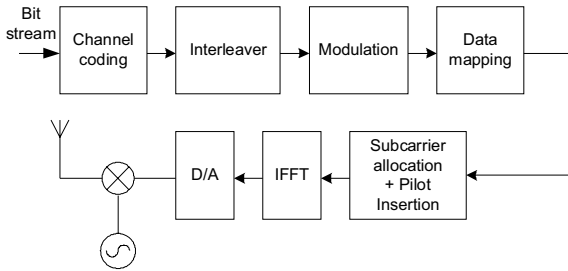


Figure 1. Mobile WiMAX functional stages

The channel coding stage includes randomization, convolutional coding (native code rate is 1/2) and puncturing to produce higher code rates. A block interleaver is used to interleave the encoded bits onto separated subcarriers, thus minimizing the impact of burst errors. Once the data has been modulated (using QPSK, 16QAM, or 64QAM), the data is mapped by segmenting the sequence of modulated symbols into a sequence of slots (using the minimum data allocation unit) and then mapping these slots into a data region. After this data mapping the modulation symbols are assigned to their corresponding logical subcarriers. These logical subcarriers are allocated to physical subcarriers using a specific sub-carrier permutation. Pilots are also inserted at this point. The final stage is to convert the data into a time-domain analogue form for use by the radio front end. A guard interval is also inserted at this stage. The reader can refer to [3] for a more detailed explanation of the above steps.

Our simulator supports a number of link-speeds (see Table III for details). A link-speed is defined by a combination of a modulation scheme and a coding rate.

TABLE III. DOWNLINK MOBILE WIMAX LINK SPEEDS

Modulation and Code Rate	No. of coded bits per subchannel	No. of data bits per subchannel	DL bit rate/user (Mbps)
QPSK 1/2	48/32	24/16	1.17
QPSK 3/4	48/32	36/24	1.75
16 QAM 1/2	96/64	48/32	2.33
16 QAM 3/4	96/64	72/48	3.50
64 QAM 1/2	144/96	72/48	3.50
64 QAM 2/3	144/96	96/64	4.66
64 QAM 3/4	144/96	108/72	5.25

III. WIDEBAND CHANNEL MODEL

The channel model used in our simulation is based on the spatial channel model (SCM) [4]. This model was developed by ETSI 3GPP-3GPP2 to help standardise the outdoor evaluation of mobile systems. The 3GPP SCM defines three typical cellular environments, namely urban macrocell (cell radius less than 1.5 km, BS antenna well above rooftop level), suburban macrocell (cell radius less than 1.5km, BS antenna well above local cluster), and urban microcell (cell radius less than 500 meters, BS antenna at rooftop level).

Based on the above 3GPP-SCM channel model, an urban micro 3GPP tapped delay line (TDL) channel model is generated for use in our analysis. The TDL includes 6 taps with non-uniform delays. The mobile station (MS) velocity is assumed to be 40 km/h. The channel has the following parameters:

TABLE IV. 3GPP TDL CHANNEL PARAMETER

	Tap 1	Tap 2	Tap 3	Tap 4	Tap 5	Tap 6
Delay (ns)	0	210	470	760	845	910
Power (dB)	0	-1.8	-1.5	-7.2	-10	-13
K factor	0	0	0	0	0	0
Delay spread	279 ns					

IV. SIMULATION PERFORMANCE ANALYSIS

In this section we present results from our Mobile WiMAX simulator using the 3GPP channel model. On the DL a 3-sector base station (BS) is assumed to transmit data to 3 MS, which each share a common OFDMA symbol. Perfect channel estimation and synchronisation is assumed at the receiver.

Fig. 2 shows the downlink PER for the urban micro channel scenario. We observe that all the curves corresponding to the same code rate have the same slope and for each modulation scheme the slope reduces with higher code rate. Another observation is that modulation schemes using the 3/4 code rate offer very poor performance; e.g., 16QAM 1/2 rate and 64QAM 1/2 rate give better performance than QPSK 3/4 rate and 16QAM 3/4 rate respectively. This poor performance can be traced to the high puncture pattern.

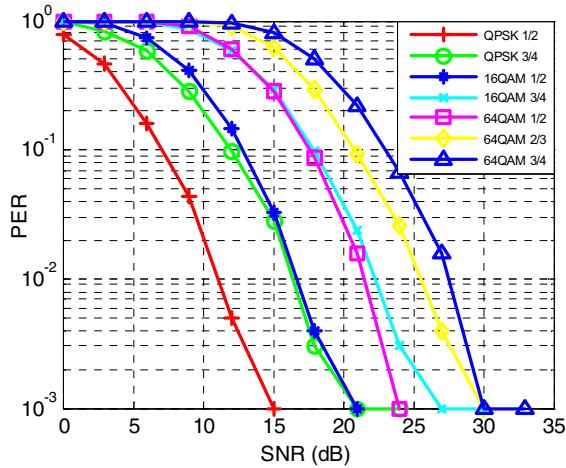


Figure 2. PER of DL WiMAX System (3GPP SCM urban micro)

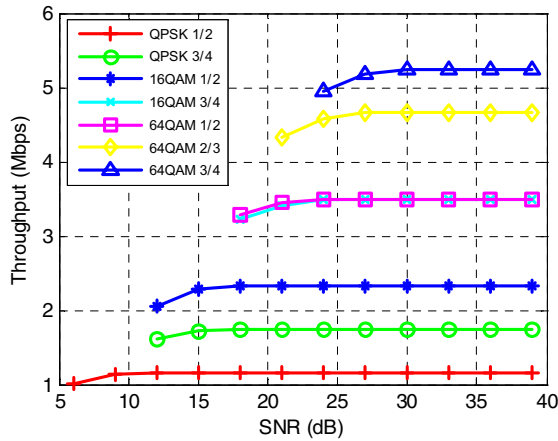


Figure 3. DL WiMAX throughput

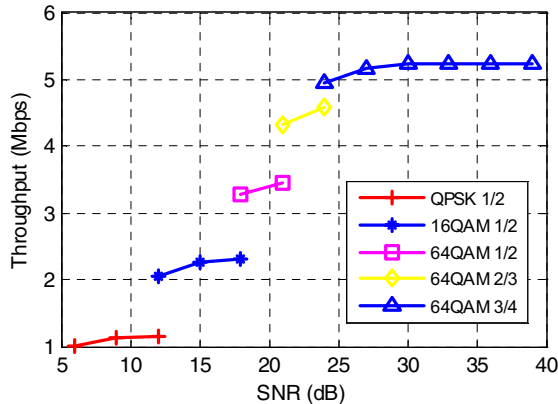


Figure 4. DL WiMAX throughput envelope

The link throughput for different link-speeds is shown in Fig. 3. The link throughput for each user is calculated from the PER as follows:

$$R = D(1 - \text{PER}) \quad (1)$$

where $D = N_D N_b R_{FEC} / T_s$ represents the peak error-free transmission rate and N_D , N_b , R_{FEC} , and T_s denote the number of assigned data subcarriers, the bits per sub-carrier, the FEC coding rate, and the OFDMA symbol duration respectively.

Any PER in excess of 10% is assumed to be too severe to maintain a practical data link and is not included in the throughput calculation. Due to the 10% PER threshold we can see that each link-speed has a minimum SNR value below which it cannot operate (e.g. 1/2 rate 16QAM can only operate at a minimum SNR of 12 dB, below this point the resulting PER will be higher than 10%).

Fig. 4 shows the DL WiMAX throughput versus SNR envelope when applying link adaptation. The envelope was generated using adaptive modulation and coding (AMC) to increase and/or decrease the link-speed to maximise the throughput for any value of SNR. As the received SNR increases it can be seen that the system ‘jumps’ to a higher link-speed in order to maximise the achievable throughput.

V. EXPERIMENTAL CONFIGURATION

The experimental data was captured using a laptop computer and a mobile WiMAX data card (see left-hand side of Fig. 5) connected to a commercial carrier-class WiMAX base-station (BS) operating at 2.3GHz. The BS used time division duplex (TDD) with scheduling based on a Round-Robin technique. The PHY layer used 1024 sub-carriers configured in a 10 MHz bandwidth. The ratio between the downlink and uplink was 80:20 in favour of the downlink. The BS power amplifier was connected via 30m of RF cable to a 2 dBi dipole antenna. This was then mounted on the roof of a two-storey building (see right-hand side of Fig. 5). An EIRP of 32dBm (including cable losses) was used at the BS.

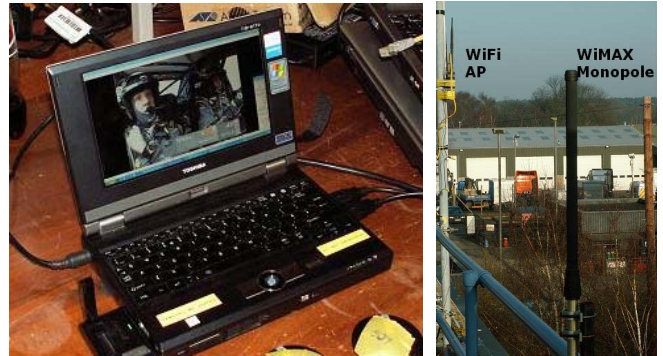


Figure 5. Mobile Laptop (left); and BS Monopole (right)



Figure 6. Mobile WiMAX enabled Laptop in Vehicle

A video server was used to compress a composite video source into an IP encapsulated H.264 stream. This was then sent over the WiMAX network via an Ethernet connection to the BS. As shown in Fig. 6 the laptop was placed inside a GPS enabled vehicle and driven in the vicinity of the WiMAX BS at

speeds of up to 35 km/h. The H.264 video was received in the moving vehicle and decoded on the laptop. The drive test involved passing through the radio shadow of numerous tall buildings. The experiment also included the logging of PER, data throughput and signal level in addition to GPS location (which was used to determine the BS-MT separation distance).

The propagation environment around the BS could be classified as urban micro. It consisted mainly of large office and industrial buildings (with heights ranging from 5m to 30m). Several housing developments and a number of open fields were located around 400m from the BS (a photograph of the test site is shown in Fig. 7). The BS antenna was located at the centre of the circles shown. This location was chosen due to its close proximity to the rack of BS equipment. The outer blue circle indicates a range of 400m from the base-station. The inner red circle indicates a range of 260m from the base-station.

VI. COMPARISON OF SIMULATED AND EXPERIMENTAL RESULTS

The downlink PER performance is based on 2500 data samples collected at the laptop while driving in the vicinity of the BS. In all cases the laptop received a broadcasted video stream over the WiMAX link. The routes used in this experiment were carefully chosen to cover a wide range of different locations, whilst ensuring that the vehicle remained within the cell boundary. Fig. 7 shows the PER at various points around the basestation. The small coloured discs indicate the level of PER (with red denoting zero PER).

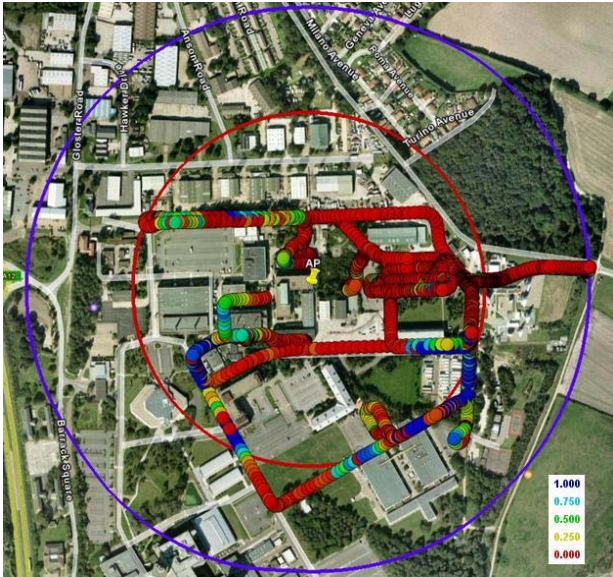


Figure 7. PER vs. location and distance for WiMAX Downlink

Fig. 8 shows the path loss exponent at different locations around the trial site. The path loss exponent n was extracted from the experimental data using Erceg's empirically based model [7], which can be written as:

$$PL = 10n \log d/d_0 + 20 \log(4\pi d_0/\lambda) \quad (2)$$

where d and d_0 represent the BS-MT separation distance and the reference distance (set to 1 m) respectively. We can see that at a range of around 300m, the value for n is typically around 3.4. This relatively low operating range is a result of urban environment, the dipole antenna and the low EIRP used at the BS (typically up to 61dBm [6] is permitted by OFCOM). Fig. 9 shows the predicted range versus throughput envelope using the link adaptation SNR thresholds shown in Fig. 4. We see that the maximum range from our WiMAX simulator is also around 300 metres when operating at the lowest link-speed, i.e. 1/2 rate QPSK. This result agrees with the experimental result. The operating range d was derived from the link budget equation (1) below:

$$SNR = (P_T G_T G_R / kTB\eta) (\lambda/4\pi)^2 (1/d)^n \quad (3)$$

$$d = [(P_T G_T G_R / kTB\eta) (\lambda/4\pi)^2 (1/SNR)]^{1/n} \quad (4)$$

where the transmit power $P_T = 30$ dBm, the transmit antenna gain $G_T = 2$ dBi, the receive antenna gain $G_R = 0$ dBi, the noise temperature $T = 290$ K, the bandwidth $B = 10$ MHz, the noise figure $\eta = 6$ dB, the carrier wavelength $\lambda = 0.1304$ m (assuming a carrier frequency $f = 2.3$ GHz), and Boltzmann's constant $k = 1.38 \times 10^{-23}$ J/K/Hz. The path loss exponent n is 3.4.

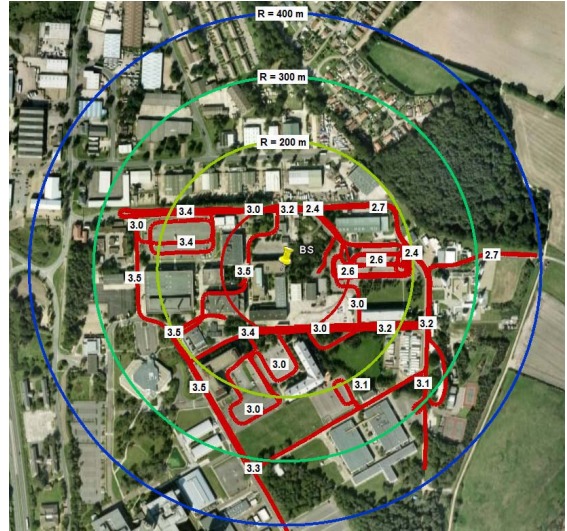


Figure 8. Estimated pathloss exponents at different spots

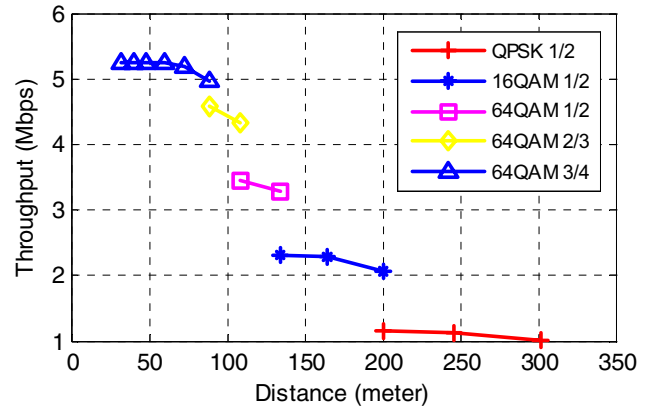


Figure 9. Simulation mobile WiMAX operating range

If a high-gain sectorised antenna (typically 16dBi) were used at the BS then the operating range would be greatly improved. Furthermore, range would be enhanced by increasing the power to the antenna port to the regulatory maximum. In the UK, operation in the licensed 2GHz band permits an EIRP for a 10MHz signal of up to 61 dBm [6]. Assuming the BS is able to supply 45dBm to the port of a 16dBi antenna, the downlink range is predicted to increase to 2.1 km as illustrated in Fig. 10

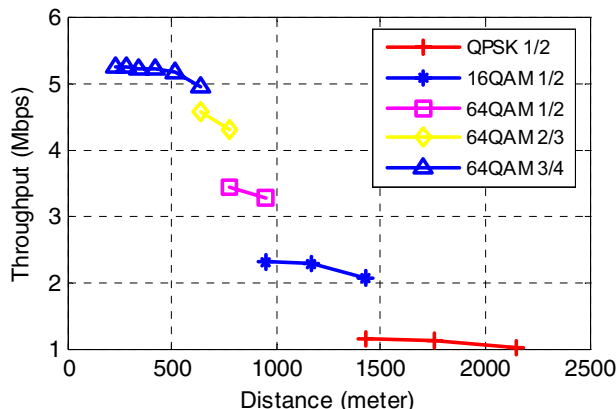


Figure 10. Simulation operating range at EIRP of 61 dBm

Fig. 11 shows a comparison between the experimental DL PER performance and the predicted performance using our mobile WiMAX simulator (based on parameters given in section II and the channel model described in section III). It should be noted that the WiMAX basestation includes link adaptation as a function of SNR. Hence, for the experimental data the PER curve correspond to different link-speeds at different SNR levels. The SNR values given in the legend of figure 11 indicate the SNR range over which each link-speed was predicted to operate. For example, the measured PER at an SNR of 13 dB should be compared with the simulated PER for the 3/4 rate 16QAM link-speed.

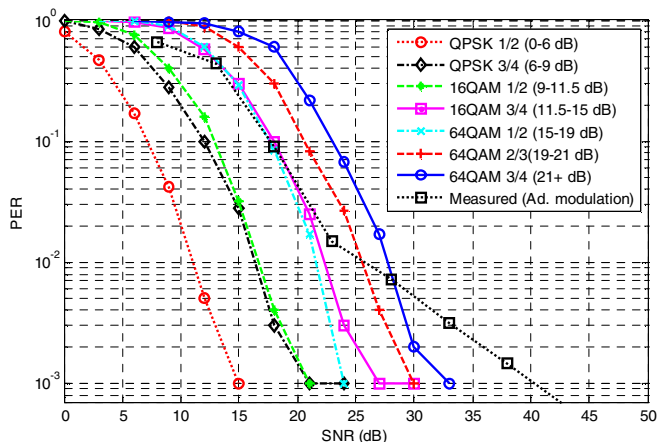


Figure 11. Experimental vs. Simulation PER comparison

It is clear from the above comparison that a good agreement has been achieved between the measured and simulated data. The greatest discrepancy occurs at the highest SNR values.

These values are estimated without considering the impact of power control in the hardware. In practice, for SNR values beyond 21dB the BS is expected to lower its transmit power, thus reducing the observed SNR.

VII. CONCLUSIONS

This paper has presented a theoretic study of the Mobile WiMAX physical layer using the well-known 3GPP spatial channel model. The simulation was fully compliant to the 802.16e-2006 standard. PER and throughput results were presented for each link-speed on the DL.

The simulated results were compared with measured drive-test results from a carrier-class WiMAX basestation. This involved driving around the basestation and logging data using a laptop computer. The final comparison (PER vs SNR) shows excellent agreement, indicating that the simulator can be used to predict performance for a range of environments, transmit power levels, and antenna configurations.

Analysis demonstrated that the street level operating range for a 2.3GHz mobile WiMAX system can be up to 2100m, depending on the basestation EIRP.

ACKNOWLEDGEMENTS

The authors would like to thank the Technology Strategy Board (TSB) for part-funding this work under the VISUALISE project. Mai Tran would also like to recognise the financial assistance provided by his Overseas Research Studentship.

REFERENCES

- [1] IEEE Std 802.16TM-2004, "Part 16: Air interface for fixed broadband wireless access systems," Oct 2004.
- [2] IEEE Std 802.16Etm-2005, "Part 16: Air interface for fixed and mobile broadband wireless access systems," Feb. 2006
- [3] M. Tran, A. Doufexi and A.R. Nix, "Mobile WiMAX MIMO Performance Analysis: Downlink and Uplink", accepted for PIMRC 2008.
- [4] 3GPP TR 25.996 v6.1.0, "Spatial channel model for Multiple Input Multiple Output (MIMO) simulations," Sep. 2003.
- [5] V. Erceg, L. Greenstein, D. Tjandra, S. Parkoff, A. Gupta, B. Kulic, A. Julius and R. Bianchi, "An Empirically Based Path Loss Model for Wireless channels in Suburban Environments", IEEE Journal on Selected Areas in Communications, Vol 17, pp. 1205-1211, 1999
- [6] Ofcom, "Award of available spectrum:2500-2690 MHz, 2010-2025 MHz and 2290-2300 MHz", Dec 2006
- [7] V. Erceg, et al, "An Empirically Based Path Loss Model for Wireless channels in Suburban Environments", IEEE Journal on Selected Areas in Communications, Vol 17, pp. 1205-1211, 1999